Acta Cryst. (1960). **13**, 575

The Crystal Structure of the *R* Phase, Mo–Co–Cr.*

BY YUKITOMO KOMURA,† WILLIAM G. SLY,‡ AND DAVID P. SHOEMAKER

Department of Chemistry, Massachusetts Institute of Technology, Cambridge, Massachusetts, U.S.A.

(*Received* 19 *June* 1959 *and in revised form* 18 *November* 1959)

The crystal structure of the *R* phase in the Mo–Co–Cr system, with atom ratio 30·4–51·3–18·3, has been determined by single-crystal X-ray diffraction analysis. The crystal has space group C_{3i}^2–$R\bar{3}$, with 53 atoms per rhombohedral cell. The rhombohedral lattice constants are $a_0 = 9{\cdot}011$ Å, $\alpha = 74° 27{\cdot}5'$, hexagonal lattice constants $a_0 = 10{\cdot}903$, $c_0 = 19{\cdot}342$ Å. The structure is closely related to those of other transition-group phases such as the σ phase (Fe–Cr and many other systems), *P* phase (Mo–Ni–Cr and Mo–Ni–Fe), χ phase (α-Mn, Mo–Fe–Cr), and μ phase (Mo–Co and other systems). The *R* phase field lies directly between the σ and μ phase fields on the Mo–Co–Cr ternary phase diagram. The *R* phase exhibits 12-fold (icosahedral), 14-fold, 15-fold, and 16-fold atomic coordination, which are the coordinations shown in various combinations by the other phases mentioned. Like the others (except χ), the *R* phase has exclusively tetrahedral interstices. As with the *P* and σ phases, but to a somewhat lesser degree, interatomic distances in the *R* phase agree with sums of characteristic radii, which are different for five- and six-coordinated ligands for each type of coordination. As in the case of the *P* phase, the molybdenum content of the atomic sites increases with coordination from approximately zero for coordination 12 to approximately 100% for coordination 16.

Introduction

The present investigation was carried out as a part of a program concerned with the investigation of the structures of some phases found in ternary systems of transition group elements by Beck and coworkers (Rideout *et al.*, 1951). These and other phases which appear to be interrelated in their structural features and phase behavior include the σ phase (Fe–Cr, Co–Cr, and many other systems), the *P* phase (Mo–Ni–Cr, Mo–Ni–Fe), the delta phase (Mo–Ni), the μ phase (Mo–Co and other systems), the χ phase (α-Mn, Mo–Fe–Cr). (References for these structures are cited by Shoemaker, Shoemaker & Wilson, 1957.) The β-tungsten and Laves–Friauf phases ($MgCu_2$, $MgZn_2$, $MgNi_2$) have structures that are less complex than the others cited, but related to them. Most of these phases appear to merit the designation of 'electron compound', since for a given structure the atomic composition is roughly determined by the electron content.

On the Mo–Co–Cr phase diagram at 1200 °C., the *R* phase, with atom ratio in the neighborhood of 30–49–21, lies between a σ phase at about 0–32–68 to 20–48–32 and a μ phase at about 36–49–14 to 48–52–0. The *R* phase, like the *P* phase, was discovered by Beck and coworkers (Rideout *et al.*, 1951).

Through the kindness of Prof. Paul A. Beck of the University of Illinois, specimens of *R* phase, with atom ratio 30·4–51·3–18·3 (by chemical analysis), annealed many hr. at 1200 °C., were made available to us for the X-ray crystallographic study here described. Some preliminary results have already been reported (Komura, Shoemaker & Shoemaker, 1957).

Unit cell and space group

In this work, as in the previous work on the σ and *P* phases, it was necessary to select many very small fragments from the pulverized alloy, mount them, and examine them by Laue photography in order to find and orient single crystals. A procedure frequently useful in the absence of morphological clues to symmetry and orientation is to take Laue photographs at a succession of trial azimuths until a mirror plane is encountered. In the present instance no mirror was found; with the weak patterns obtained (even after 24 hr. exposure) it was even difficult to determine whether fragments examined were single crystals, until by accident similar patterns were obtained with two different fragments, and later with two different settings of one fragment. The latter finding led to the discovery of a three-fold rotation axis. No Laue symmetry was found higher than C_{3i}–$\bar{3}$, the only centrosymmetric class besides C_i–$\bar{1}$ that has no mirror plane. All later single crystal work was done with one fragment, a tiny flake less than 0·05 mm. in its longest dimension, mounted on a glass fiber with fused shellac.

The lattice was established as rhombohedral with the aid of a gnomonic projection of a Laue photograph. With Weissenberg and oscillation photographs the axial lengths were obtained, although very few re-

* Sponsored by the Office of Ordnance Research. The computations were in large part done at the M.I.T. Computation Center.

† Present address: Department of Chemistry, Institute of Polytechnics, Osaka City University, Osaka, Japan.

‡ Present address: Department of Chemistry, Harvey Mudd College, Claremont, California.

Table 1. *Powder photographic data**

hkℓ	$\frac{1}{d_{cal}}$	I_{cal}	$\frac{1}{d_{obs}}$	I_{obs}†
131	.3854	3.1	.3847	f
312	.3956	4.3		
223	.3983	6.22		
027	.4193	1.8	.4194	vf
			.4217	f
401	.4268	1.6	.4275	vw
018	.4269	18.4		
134	.4344	11.0	.4350	f
042	.4361	1.8		
306	.4440	6.8	.4463	vf
217	.4577	78.4	.4581	vs
315	.4611	84.0	.4614	vs
321	.4646	.5	.4670	vw
208	.4647	4.2		
404	.4714	9.1		
232	.4731	70.5	.4734	vs
226	.4804	1.9		
410	.4854	62.2	.4857	vs
045	.4963	46.4	.4960	s
128	.4996	51.4	.5008	vs
119	.5001	33.6		
324	.5059	36.9	.5056	m
413	.5095	28.8	.5080	w
137	.5261	8.8	.5217	vf
1.0.10	.5277	15.1	.5289	mw
235	.5291	12.6		
051	.5321	2.5		
502	.5396	9.7	.5382	vw
0.2.10	.5587	0.6	.5575	vw
241	.5628	2.3	.5624	w(b)
309	.5634	16.2		
054	.5685	2.1	.5690	w
333	.5718	2.5		
416	.5760	8.6	.5764	f(b)
0.1.11	.5784	0.5	.5800	f
		**		
3.0.12	.6970	2.0	.6985	f(b)
612	.7022	8.0	.7031	f(b)
0.2.13	.7046	1.8		
606	.7071	4.4		
0.4.11	.7091	3.2		
			.7157	w(b)
158	.7203	0.9		
339	.7207	4.2		
526	.7306	9.5		
0.1.14	.7314	5.9	.7318	w
2.3.11	.7325	2.4		
0.5.10	.7401	0.9		
701	.7432	5.2	.7432	f(b)
443	.7500	1.5	.7499	f
2.0.14	.7541	0.6	.7510	f(b) ?
2.4.10	.7625	0.6	.7587	f(b) ?
			.7625	f(b) ?
348	.7656	1.0	.7667	f
704	.7697	8.7	.7698	vw
262	.7707	2.3		
0.0.15	.7754	6.3	.7726	f ?
1.2.14	.7761	17.5	.7780	mw
5.1.10	.7842	1.4	.7848	w
535	.7852	20.3		
609	.7876	15.4	.7876	mw
4.1.12	.7877	16.5		
624	.7913	1.3	.7987	w
1.1.15	.7968	1.3	.7972	f
4.2.11	.7984	3.8		
710	.7996	22.7	.7998	vw
			.8029	f(?)
265	.8063	12.6	.8074	f
618	.8083	1.8	.8098	ms
529	.8087	29.1		
713	.8145	23.9	.8162	s
3.2.13	.8153	10.5		
3.1.14	.8183	6.7	.8189	vf
1.5.11	.8192	1.4		
			.8211	f
707	.8250	12.1	.8264	w
4.3.10	.8260	6.7		
541	.8288	8.0	.8313	f
3.3.12	.8293	5.4		
452	.8337	1.5		
1.0.16	.8339	2.1		
3.0.15	.8380		.8376	mw
630	.8407	5.3	.8408	w
627	.8452	1.0	.8450	vf
081	.8489	5.2	.8498	vvf

*hkℓ: based on hexagonal axes

$1/d_{cal}$: from final lattice constants

$I_{cal} = KmF^2$: from single-crystal intensity data

$1/d_{obs}$: average of FeKα and CrKα data

I_{obs}: average powder-line intensity

** No significant lines predicted, and none observed, in this range

† s = strong, m = medium, w = weak, f = faint, b = broad, v = very

flections were observed on the equatorial Weissenberg photograph.

The lattice constants were eventually refined with powder data obtained with Fe $K\alpha$ and Cr $K\alpha$ radiation. The powder lines, measured from photographs taken on a 114·59 mm. Philips powder camera (Straumanis arrangement), were indexed with the aid of a predicted powder diagram based on three-dimensional single-crystal intensity data, and the lattice constants were refined by least squares by the procedure used for the *P* phase (Shoemaker, Shoemaker & Wilson, 1957). The powder data are given in Table 1. The final values of the lattice constants are:

Rhombohedral	Hexagonal
$a_0 = 9{\cdot}011 \pm 0{\cdot}005$ Å	$a_0 = 10{\cdot}903 \pm 0{\cdot}005$ Å
$\alpha = 74° 27{\cdot}5' \pm 2'$	$c_0 = 19{\cdot}342 \pm 0{\cdot}011$ Å

The density was measured by displacement in a pycnometer. Six independent measurements yielded an average value of 9·011 g.cm.$^{-3}$ with an average deviation of 0·013. With the given composition this corresponds to 50·92 atoms per rhombohedral cell, suggesting the number 51. Our experience with the *P* phase (which apparently had a density lower than the calculated value because of slag inclusions) suggested that the number of atoms could be higher—52, 53, or even possibly 54.

The only two space groups compatible with the rhombohedral lattice and the observed Laue symmetry are $R3$ and $R\bar{3}$. The latter was provisionally assumed in the subsequent work, and eventually found to be the correct one.

Determination of the structure

The provisionally assumed space group $R\bar{3}$ has two sets of 3-fold special positions, but these did not appear to be occupied since peaks required by them in the basal plane Patterson projection (Fig. 1) are not observed. The only other special positions lie on the three-fold rotation axes. The general positions in this space group are 6-fold. With 51 to 53 atoms per rhombohedral cell (with a 19·3 Å hexagonal **c**-repeat) it is clear that three to five must lie on the three-fold axis. With 54 atoms, the number could be either zero or six. However, if there are no atoms on the axis, or indeed any fewer than four per cell, it is clear that

interstices must be present on the axis that are not tetrahedral. Although a few models with one or a few octahedral interstices were examined, the virtual absence of other than tetrahedral interstices in the other known transition alloy complex structures made it seem probable that only tetrahedral interstices are present in the R phase. Thus it appeared that there are four, five, or perhaps six atoms on the axis per unit cell.

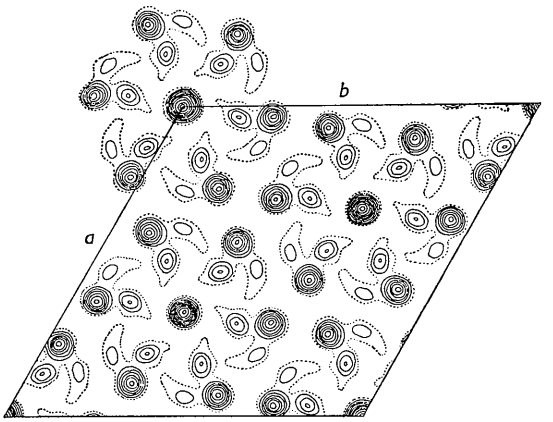

Fig. 1. Patterson projection on basal plane.

This circumstance requires that four to six atoms be superimposed in projection on the basal plane, making it probable that in such a projection they behave like a single 'heavy atom', making the signs positive for most or all of the large structure factors in the $(hk0)_{hex}$ zone. The basal plane Patterson projection (Fig. 1) should therefore be expected to resemble closely an electron-density projection of the structure. In this projection a cluster of peaks surround the origin and other lattice points. The strong peaks in each cluster suggest immediately a projection of a regular icosahedron.

These considerations led us to consider possible configurations of icosahedra, and other of the coordination polyhedra that were encountered in the σ and P phases, with their four, five or six central atoms on the three-fold axis, and with sharing of vertices or faces.

After a number of trials, a promising arrangement was found with five atoms. This consisted of three icosahedra and two CN 16 polyhedra (octicosahedra), the icosahedra sharing triangular faces with each other and with the CN 16 polyhedra, and the latter mutually sharing a six-membered ring. The atoms of the CN 16 polyhedra, except for those in the six-membered ring, project together with all but one kind of icosahedral atoms ($B2$) onto the strong peaks of the Patterson projection. The weak peaks are reasonably well accounted for by the remaining atoms (6-ring and $B2$).

The chain of polyhedra accounts for one one-fold and two two-fold sets of special positions, and eight six-fold sets of general positions, totalling 53 atoms

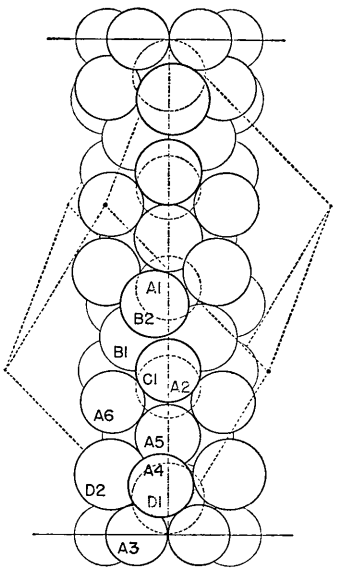

Fig. 2. R phase structure: chain of packing polyhedra along three-fold axis.

per rhombohedral cell. The structure consists of such chains packed together, one running along each three-fold axis. Two configurations for the chain, related by a reflection in the basal plane or a 60° rotation, had to be considered; the construction of models of both showed clearly that one and only one of them yields a plausible structure from the packing standpoint. In this one, it was possible to identify the coordinations of all of the atoms in terms of the CN 12, 14, 15, and 16 polyhedra previously encountered in the σ and P phases. Moreover, this structure yielded three-dimensional calculated structure factors in reasonable agreement with the observed. The chain is shown in its correct configuration, in relation to the rhombohedral unit cell, in Fig. 2.

Parameter refinement

Intensity data for refinement were obtained by visual estimation of intensities of diffraction spots on multiple-film equi-inclination Weissenberg photographs, with the aid of intensity strips, in the usual way. The crystal was rotated around the three-fold axis for layers $l=0$ to $l=16$, and around $[110]_{hex.}$ for the first five layers. Copper $K\alpha$ radiation was used. Owing in part to the smallness of the crystal (and despite exposures of 150–200 hr.), but also in large part to the rather unusual distribution of intensities that is peculiar to structures of this kind, 521 of the 900 nonequivalent planes accessible to observation were too weak to be observed.

Because at the time the approximate structure was obtained our computing facilities for least-squares refinement were not yet ready, an interim attempt was made to obtain some 'refinement' without recourse to intensity data, by attempting to minimize devia-

tions between interatomic distances calculated from atomic coordinates and distances obtained from radius sums for the corresponding polyhedra (as found for the *P* phase). This was done by a procedure tantamount to a diagonal least-squares treatment; in each cycle, the distances were calculated, and the differences between them and radius sums were averaged to obtain shifts. Six cycles were carried through to approximate convergence, accomplishing about half of the ultimate refinement; the average deviation of the parameters from their final values was reduced from 0·0084 to 0·0039. These calculations were of value in showing that the structural geometry itself imposes certain limits on the degree of ultimate agreement between actual distances and radius sums, since a number of large (0·1–0·2 Å) deviations remained after this treatment; these were, for the most part, for the same atom pairs for which large distance deviations were found after ultimate refinement with X-ray intensities.

Intensity refinement was carried out by the method of least squares on the IBM 704 computer, with the program NY XR 1 developed by D. Sayre and modified by V. Vand. This program omits off-diagonal normal-equation coefficients. All observations included in the refinement were weighted equally. In the early stages, all planes accessible to observation were included, but in the later stages the unobserved planes were omitted. Also omitted in the later stages were twenty-three reflections which seemed liable to suspicion of abnormal error or mis-identification. All of these were observed considerably stronger than calculated, and most were near the edge of the sphere of reflection. As the films contain many random spots clearly due to misoriented attached crystal fragments, it is likely that some such spots were mistaken for spots due to the main crystal.

To determine approximately the occupancy of atomic sites with molybdenum atoms, some refinement with respect to 'atomic numbers' or 'atomic scale parameters' for the several kinds of atomic sites was carried out. This was done with a modification of NY XR 1, in which these parameters replaced the temperature factor parameters.

Following thirteen cycles of preliminary refinement, and two cycles of atomic number refinement, the form factors for the various sites were adjusted in accord with the atomic numbers obtained and three additional cycles of positional and temperature factor refinement and one of temperature factor refinement alone were carried out. In these final cycles, Thomas–Fermi–Dirac (TFD) form factors (Thomas & Umeda, 1957) were used, in linear combinations of cobalt and molybdenum suggested by the atomic number results. These form factors were corrected for anomalous dispersion in accordance with the table of Dauben & Templeton (1955). The final values of the positional, temperature factor, and atomic number parameters are given in Table 2, together with the approximate molybdenum percentages assumed for calculating structure factors. The positional parameters are given in terms of the hexagonal cell ('obverse' relationship; rhombohedral lattice points at 0, 0, 0; $\frac{2}{3}, \frac{1}{3}, \frac{1}{3}$; $\frac{1}{3}, \frac{2}{3}, \frac{2}{3}$). In Table 3 the final calculated structure factors are compared with the observed. The structure factors are scaled to the 159-atom hexagonal cell. The final reliability factor, *R*, was 9·6% for the reflections included in the refinement.

Discussion

The structure, shown in various aspects in Figs. 2 to 6, is of lower symmetry than any of the other transition group alloy phases of known structure that have been here mentioned; this and its evident complexity make detailed comparisons with the other structures difficult. Some direct structural relationships with the σ phase (Bergman & Shoemaker, 1954) and *P* phase (Shoemaker, Shoemaker & Wilson, 1957) can be seen, however, by means of an axis transformation,

$$\begin{pmatrix} \mathbf{a}' \\ \mathbf{b}' \\ \mathbf{c}' \end{pmatrix} = \begin{pmatrix} \frac{2}{3} & \frac{1}{3} & \frac{1}{3} \\ -\frac{5}{3} & \frac{5}{3} & \frac{2}{3} \\ -\frac{1}{3} & \frac{1}{3} & \frac{1}{3} \end{pmatrix} \cdot \begin{pmatrix} \mathbf{a}_{\text{hex.}} \\ \mathbf{b}_{\text{hex.}} \\ \mathbf{c}_{\text{hex.}} \end{pmatrix}$$

$$= \begin{pmatrix} 1 & 0 & 0 \\ -1 & 4 & -1 \\ 0 & 1 & 0 \end{pmatrix} \cdot \begin{pmatrix} \mathbf{a}_{\text{rh}} \\ \mathbf{b}_{\text{rh}} \\ \mathbf{c}_{\text{rh}} \end{pmatrix},$$

Table 2. *Atomic parameters*

Atom	Pos.	CN	*x*	*y*	*z*	*B*	Z_o	% Mo*	$Z_{\text{assum.}}$†
*A*1	3(*b*)	12	0	0	$\frac{1}{2}$	1·72	27·3	11	26·8
*A*2	6(*c*)	12	0	0	0·3044	1·17	25·3	0	25·0
*A*3	18(*f*)	12	0·1596	0·2470	0·0020	0·59	25·0	0	25·0
*A*4	18(*f*)	12	0·0509	0·2790	0·1000	0·43	25·1	0	25·0
*A*5	18(*f*)	12	0·0212	0·1393	0·1962	1·28	26·3	11	26·8
*A*6	18(*f*)	12	0·2250	0·1969	0·2685	0·40	25·3	0	25·0
*B*1	18(*f*)	14	0·1759	0·1265	0·3969	0·59	35·2	62	35·2
*B*2	18(*f*)	14	0·1132	0·2687	0·4652	0·76	33·8	53	33·8
*C*1	18(*f*)	15	0·0330	0·2579	0·3183	0·59	37·4	76	37·5
*D*1	6(*c*)	16	0	0	0·0735	0·38	44·4	100	41·5
*D*2	18(*f*)	16	0·2671	0·2218	0·1222	0·44	41·8	100	41·5

* % Mo assumed in a linear combination of Mo and Co form factors used in calculating structure factors.
† Effective form factor at $\theta = 0$, based on % Mo assumed; 0·5 and 2·0 electrons subtracted from f_{Mo} and f_{Co} respectively.

Table 3. *Calculated and observed structure factors for R phase*

K	FCAL	FOBS
	0 K 0	
3	18	91 M
6	159	148 M
9	27	181 M
12	109	67 M
	1 K 0	
1	13	67 M
4	1572	1595
7	1321	1452
10	42	148 M
	2 K 0	
2	45	100 M
5	9	153 M
8	385	421
	3 K 0	
3	20	133 M
6	370	366
9	124	139 M
	4 K 0	
1	119	121 M
4	427	338
7	195	172 M
	5 K 0	
2	288	279
5	8	183 M
8	296	295
	6 K 0	
3	422	399
6	383	443
	7 K 0	
1	49	175 M
4	103	174 M
	8 K 0	
2	80	179 M
5	101	116 M
	9 K 0	
3	904	1039
	10 K 0	
1	148	155 M
	0 K 1	
2	11	72 M
5	131	128 M
8	110	177 M
11	43	128 M
	1 K 1	
0	6	49 M
3	244	183
6	46	157 M
9	41	174 M
	2 K 1	
1	110	86 M
4	576	565
7	647	725
10	55	124 M
	3 K 1	
- 1	83	84 M
2	60	117 M
5	56	166 M
8	125	166 M
	4 K 1	
- 3	139	102 M
0	625	586
3	11	150 M
6	103	179 M
9	80	102 M
	5 K 1	
- 2	191	116 M
1	57	141 M
4	117	175 M
7	232	152 M
	6 K 1	
- 4	585	523
- 1	194	199
2	141	168 M
5	357	406
	7 K 1	
- 6	15	157 M
- 3	100	148 M
0	143	166 M
3	288	327
6	309	305
	8 K 1	
- 5	670	545
- 2	211	220
1	58	181 M
4	107	146 M
	9 K 1	
- 7	102	177 M
- 4	599	682
- 1	612	638
2	36	159 M
	10 K 1	
- 9	311	327
- 6	84	179 M
- 3	79	177 M
0	53	163 M
3	357	322
	11 K 1	
- 8	16	166 M
- 5	69	174 M
- 2	208	287
1	146	105 M
	12 K 1	
-10	144	124 M
- 7	2	153 M
- 4	86	271
- 1	21	103 M
	13 K 1	
- 9	495	431
- 6	251	234
- 3	66	84 M
	0 K 2	
1	11	47 M
4	55	164
7	98	159 M
10	182	247
	1 K 2	
2	176	150
5	213	224
8	55	172 M
11	226	206
	2 K 2	
0	71	69 M
3	134	166
6	221	228
9	244	276
	3 K 2	
- 2	136	131
1	263	225
4	359	327
7	42	170 M
10	144	79 M
	4 K 2	
- 1	3	98 M
2	42	130 M
5	86	168 M
8	10	141 M
	5 K 2	
- 3	1750	1641
0	619	575
3	16	159 M
6	125	166 M
	6 K 2	
- 5	84	133 M
- 2	88	128 M
1	752	682
4	254	297
7	181	210
	7 K 2	
- 4	33	142 M
- 1	151	152 M
2	67	170 M
5	249	292
	8 K 2	
- 6	284	247
- 3	37	159 M
0	75	170 M
3	368	416
	9 K 2	
- 8	362	332
- 5	345	332
- 2	91	170 M
1	30	166 M
4	15	96 M
	10 K 2	
- 7	26	170 M
- 4	818	811
- 1	469	496
2	32	119 M
	11 K 2	
- 9	54	153 M
- 6	62	166 M
- 3	277	320
0	338	303
	12 K 2	
-11	325	284
- 8	173	139 M
- 5	66	142 M
- 2	88	210
	13 K 2	
-10	41	81 M
- 7	9	110 M
- 4	366	336
	0 K 3	
0	41	59 M
3	21	95 M
6	111	152 M
9	34	183 M
	1 K 3	
1	67	71 M
4	47	128 M
7	15	181 M
10	365	361
	2 K 3	
1	59	69 M
2	128	112 M
5	368	372
8	66	181 M
	3 K 3	
0	149	128
3	303	285
6	294	348
9	137	137 M
	4 K 3	
- 2	362	281
1	1004	1006
4	53	170 M
7	188	174 M
	5 K 3	
- 4	14	124 M
- 1	151	124 M
2	190	159 M
5	15	183 M
8	488	399
	6 K 3	
- 3	45	137 M
0	104	153 M
3	20	183 M
6	23	152 M
	7 K 3	
- 5	85	159 M
- 2	197	197
1	725	716
4	482	499
	8 K 3	
- 7	42	181 M
- 4	302	267
- 1	116	411
2	44	181 M
5	312	285
	9 K 3	
- 6	484	392
- 3	39	183 M
0	186	183 M
3	92	137 M
	10 K 3	
- 8	165	181 M
- 5	88	183 M
- 2	327	331
1	117	157 M
	11 K 3	
-10	144	150 M
- 7	152	174 M
- 4	374	382
- 1	148	148 M
	12 K 3	
- 9	26	139 M
- 6	110	153 M
- 3	153	137 M
	13 K 3	
- 8	190	213
- 5	135	110 M
	0 K 4	
2	11	129
5	290	258
8	80	166 M
11	221	239
	1 K 4	
0	85	47 M
3	451	390
6	348	287
9	639	618
	2 K 4	
1	96	81 M
4	199	128 M
7	156	168 M
10	179	185
	3 K 4	
- 1	195	148
2	1286	1206
5	287	260
8	21	159 M
	4 K 4	
- 3	235	279
0	496	448
3	106	144 M
6	479	538
9	124	88 M
	5 K 4	
- 2	91	110 M
1	51	133 M
4	37	166 M
7	432	464
	6 K 4	
- 4	27	128 M
- 1	9	153 M
2	12	161 M
5	234	290
	7 K 4	
- 6	314	278
- 3	23	142 M
0	125	159 M
3	4	166 M
6	1	103 M
	8 K 4	
- 5	842	686
- 2	235	255
1	579	589
4	5	132 M
	9 K 4	
- 7	63	168 M
- 4	81	166 M
- 1	313	346
2	605	516
	10 K 4	
- 9	283	308
- 6	955	832
- 3	63	166 M
0	2	148 M
3	97	65 M
	11 K 4	
- 8	0	153 M
- 5	32	159 M
- 2	238	273
1	179	91 M
	12 K 4	
-10	905	444
- 7	88	137 M
- 4	223	258
- 1	97	91 M
	13 K 4	
- 9	44	93 M
- 6	294	293
- 3	563	325
	0 K 5	
1	42	45 M
4	1501	1340
7	9	157 M
10	97	146 M
	1 K 5	
2	24	82 M
5	189	133 M
8	610	548
11	441	336
	2 K 5	
0	17	69 M
3	746	657
6	552	507
9	81	141 M
	3 K 5	
- 2	287	222
1	189	100 M
4	227	142 M
7	172	164 M
	4 K 5	
- 1	1720	1768
2	21	130 M
5	39	166 M
8	38	126 M
	5 K 5	
- 3	138	112 M
0	289	274
3	1406	1347
6	628	711
	6 K 5	
- 5	128	133 M
- 2	21	128 M
1	5	152 M
4	71	166 M
7	655	618
	7 K 5	
- 4	113	142 M
- 1	147	150 M
2	21	146 M
5	11	152 M
	8 K 5	
- 6	833	761
- 3	200	157 M
0	44	166 M
3	84	148 M
	9 K 5	
- 8	7	166 M
- 5	653	625
- 2	269	318
1	349	372
4	124	82 M
	10 K 5	
- 7	132	164 M
- 4	5	166 M
- 1	181	153 M
2	442	592
	11 K 5	
- 9	295	273
- 6	161	155 M
- 3	124	148 M
0	96	110 M
	12 K 5	
-11	127	84 M
- 8	23	126 M
- 5	519	467
- 2	572	535
	13 K 5	
- 7	188	192
- 4	51	139 M
	0 K 6	
0	30	86 M
3	363	300
6	75	163 M
9	124	181 M
	1 K 6	
1	215	155
4	333	332
7	147	185 M
10	23	137 M
	2 K 6	
- 1	87	74 M
2	43	110 M
5	823	757
8	91	177 M
	3 K 6	
- 2	196	191
1	39	133 M
4	41	177 M
7	57	168 M
	4 K 6	
- 4	313	321
- 1	302	274
2	85	166 M
5	211	185 M
8	0	95 M
	5 K 6	
- 3	56	146 M
0	506	475
3	163	187 M
6	191	278
	6 K 6	
- 5	90	166 M
- 2	0	166 M
1	67	185 M
4	140	168 M
	7 K 6	
- 7	256	298
- 4	253	258
- 1	165	185 M
2	47	177 M
5	54	95 M
	8 K 6	
1	166	144
4	154	179
7	500	459
10	551	520
	9 K 6	
- 6	96	187 M
- 3	15	187 M
0	176	243
3	62	126 M
	10 K 6	
- 8	264	287
- 5	322	344
- 2	42	177 M
1	73	137 M
	11 K 6	
-10	333	318
- 7	71	168 M
- 4	31	166 M
- 1	145	137 M
	12 K 6	
- 9	123	128 M
- 6	362	344
- 3	59	126 M
	13 K 6	
- 8	139	96 M
- 5	156	179
	0 K 7	
2	198	152
5	30	121 M
8	184	230
11	285	247
	1 K 7	
0	81	141
3	36	98 M
6	132	146 M
9	112	139 M
	2 K 7	
1	1842	1639
4	291	255
7	70	155 M
10	132	86 M
	3 K 7	
- 1	56	81 M
2	54	110 M
5	558	571
8	394	433
	4 K 7	
- 3	585	523
0	18	103 M
3	87	139 M
6	64	152 M
	5 K 7	
- 2	95	110 M
1	210	202
4	211	264
7	163	116 M
	6 K 7	
- 4	381	331
- 1	122	130 M
2	51	152 M
5	373	357
	7 K 7	
- 6	120	144 M
- 3	10	137 M
0	667	677
3	417	511
6	181	165
	8 K 7	
- 5	66	150 M
- 2	22	153 M
1	32	153 M
4	215	199
	9 K 7	
- 7	766	725
- 4	354	377
- 1	173	153 M
2	33	124 M
	10 K 7	
- 9	120	141 M
- 6	61	152 M
- 3	250	271
0	756	791
	11 K 7	
- 8	97	132 M
- 5	143	139 M
- 2	97	124 M
	12 K 7	
-10	70	88 M
- 7	195	209
- 4	50	110 M
- 1	223	112
	13 K 7	
- 6	212	179
	0 K 8	
1	166	144
4	154	179
7	500	459
10	551	520
	1 K 8	
2	136	129
5	242	213
8	86	141 M
	2 K 8	
0	131	96
3	119	103 M
6	28	141 M
9	198	110 M
	3 K 8	
- 1	1447	1452
1	312	264
4	36	130 M
7	86	137 M
	4 K 8	
- 1	28	91 M
2	182	224
5	381	409
8	278	287
	5 K 8	
- 3	2	103 M
0	105	114 M
3	17	141 M
6	56	126 M
	6 K 8	
- 5	84	123 M
- 2	194	189
1	330	307
4	9	141 M
7	82	110
	7 K 8	
- 4	129	130 M
- 1	24	135 M
2	525	473
5	196	213
	8 K 8	
- 6	59	141 M
- 3	319	292
0	390	384
3	120	192
	9 K 8	
- 8	243	300
- 5	27	142 M
- 2	10	142 M
1	52	126 M
	10 K 8	
- 7	311	300
- 4	278	286
- 1	24	126 M
2	74	74 M
	11 K 8	
- 9	56	112 M
- 6	131	128 M
- 3	291	278
0	48	81 M
	12 K 8	
- 8	134	98 M
- 5	202	176
- 2	37	74 M
	13 K 8	
- 7	285	217
	0 K 9	
0	673	533
3	83	84 M
6	1267	1175
9	157	132 M
	1 K 9	
1	63	62 M
4	163	165
7	476	435
10	397	361
	2 K 9	
- 1	1106	1107
2	247	209
5	5	133 M
8	2	128 M
	3 K 9	
0	28	84 M
3	457	459
6	283	294
9	221	200
	4 K 9	
- 2	101	138
1	120	110 M
4	182	139 M
7	108	117 M
	5 K 9	
- 4	21	110 M
- 1	160	175
2	311	267
5	522	641
	6 K 9	
- 3	16	119 M
0	33	130 M
3	167	141 M
6	165	96 M
	7 K 9	
- 5	244	229
- 2	1539	1617
1	200	222
4	86	117 M
	8 K 9	
- 7	58	141 M
- 4	37	139 M
- 1	463	490
2	446	465
	9 K 9	
- 6	18	141 M
- 3	72	141 M
0	207	252
3	3	79 M

Table 3 (*cont.*)

10 K 9

- 8	124	128	M
- 5	95	137	M
- 2	25	128	M
1	27	91	M

11 K 9

-10	35	91	M
- 7	590	575	
- 4	70	117	M
- 1	14	91	M

12 K 9

- 9	123	151	
- 6	532	516	
- 3	653	596	

0 K 10

2	157	124	
5	220	202	
8	308	344	

1 K 10

0	858	734	
3	63	100	M
6	197	199	
9	134	117	M

2 K 10

1	166	220	
4	98	163	
7	715	716	

3 K 10

- 1	74	82	M
2	237	221	
5	53	144	M
8	41	110	M

4 K 10

- 3	1	154	
0	73	107	M
3	663	665	
6	315	356	

5 K 10

- 2	125	112	M
1	188	130	M
4	89	142	M
7	188	202	

6 K 10

- 4	101	126	M
- 1	300	264	
2	113	144	M
5	109	119	M

7 K 10

- 6	96	141	M
- 3	19	137	M
0	8	144	M
3	29	132	M

8 K 10

- 5	56	144	M
- 2	1000	1086	
1	239	268	
4	38	157	

9 K 10

- 7	158	248	
- 4	47	142	M
- 1	271	334	
2	572	538	

10 K 10

- 9	154	119	M
- 6	23	137	M
- 3	152	220	
0	82	105	M

11 K 10

- 8	186	226	
- 5	116	119	M
- 2	175	191	

12 K 10

- 7	170	186	
- 4	9	79	M

0 K 11

1	99	117	
4	446	395	
7	141	153	M
10	5	103	M

1 K 11

2	27	95	M
5	165	142	M
8	278	320	

2 K 11

0	181	181	
3	97	124	M
6	12	150	M
9	100	96	M

3 K 11

- 2	85	93	M
1	118	112	M
4	156	202	
7	77	135	M

4 K 11

- 1	161	172	
2	5	141	M
5	54	152	M
8	69	77	M

5 K 11

- 3	543	507	
0	55	135	M
3	627	645	
6	135	191	

6 K 11

- 5	26	141	M
- 2	120	139	M
1	102	152	M
4	517	622	

7 K 11

- 4	78	148	M
- 1	131	152	M
2	19	148	M
5	15	84	M

8 K 11

- 6	170	203	
- 3	282	248	
0	11	150	M
3	3	109	M

9 K 11

- 8	318	356	
- 5	101	153	M
- 2	67	148	M
1	140	119	M

10 K 11

- 7	56	135	M
- 4	267	310	
- 1	410	413	

11 K 11

- 9	325	329	
- 6	22	119	M
- 3	41	109	M

12 K 11

- 8	139	137	
- 5	427	387	

0 K 12

0	233	196	
3	155	114	M
6	40	166	M
9	259	320	

1 K 12

1	336	305	
4	81	146	M
7	60	166	M

2 K 12

- 1	56	82	M
2	75	124	M
5	334	304	
8	353	499	

3 K 12

0	80	116	M
3	276	262	
6	55	164	M

4 K 12

- 2	133	124	M
1	100	146	M
4	288	292	
7	400	471	

5 K 12

- 4	974	1072	
- 1	195	226	
2	171	166	M
5	42	141	M

6 K 12

- 3	640	661	
0	263	268	
3	306	392	
6	56	81	M

7 K 12

- 5	96	166	M
- 2	46	166	M
1	155	166	M
4	523	641	

8 K 12

- 7	529	568	
- 4	141	170	M
- 1	12	166	M
2	10	135	M

9 K 12

- 6	6	164	M
- 3	18	164	M
0	21	141	M

10 K 12

- 8	302	310	
- 5	148	153	M
- 2	108	135	M

11 K 12

- 7	170	234	
- 4	420	428	

12 K 12

- 6	26	81	M

0 K 13

2	321	278	
5	108	139	M
8	45	139	M

1 K 13

0	119	59	M
3	30	116	M
6	206	244	
9	82	100	M

2 K 13

1	244	209	
4	18	141	M
7	129	135	M

3 K 13

- 1	270	236	
2	1439	1471	
5	125	150	M
8	283	289	

4 K 13

- 3	40	117	M
0	106	123	M
3	43	148	M
6	742	920	

5 K 13

- 2	175	186	
1	7	144	M
4	9	141	M

6 K 13

- 4	44	141	M
- 1	27	144	M
2	225	248	
5	22	102	M

7 K 13

- 6	641	661	
- 3	620	611	
0	23	148	M
3	30	119	M

8 K 13

- 5	28	150	M
- 2	169	211	
1	512	551	

9 K 13

- 7	26	137	M
- 4	65	141	M
- 1	1	130	M
2	44	131	

10 K 13

- 9	83	102	M
- 6	390	426	
- 3	80	119	M
0	202	207	

11 K 13

- 8	418	392	
- 5	122	102	M
- 2	178	153	

0 K 14

1	228	202	
4	118	128	M
7	324	323	

1 K 14

2	9	103	M
5	14	146	M
8	114	123	M

2 K 14

0	134	154	
3	63	133	M
6	220	284	

3 K 14

- 2	1232	1220	
1	523	507	
4	116	150	M
7	221	234	

4 K 14

- 1	373	361	
2	1146	1214	
5	231	257	

5 K 14

- 3	48	133	M
0	14	141	M
3	132	146	M
6	107	88	M

6 K 14

- 5	556	513	
- 2	151	144	M
1	152	150	M
4	109	117	M

7 K 14

- 4	188	150	M
- 1	70	150	M
2	483	499	

8 K 14

- 6	26	146	M
- 3	374	404	
0	57	133	M
3	112	67	M

9 K 14

- 8	94	123	M
- 5	7	137	M
- 2	2	132	M
1	334	316	

10 K 14

- 7	708	734	
- 4	151	117	M
- 1	30	88	M

11 K 14

- 6	563	568	
- 3	577	426	

0 K 15

0	1307	1287	
3	304	300	
6	79	141	M
9	2	93	M

1 K 15

1	79	84	M
4	282	267	
7	309	298	

2 K 15

- 1	20	84	M
2	19	119	M
5	143	141	M
8	187	168	

3 K 15

0	391	366	
3	54	137	M
6	167	123	M

4 K 15

- 2	108	117	M
1	71	133	M
4	24	137	M

5 K 15

- 4	96	172	
- 1	256	208	
2	194	209	
5	84	107	M

6 K 15

- 3	172	137	M
0	44	141	M
3	15	123	M

7 K 15

- 5	348	321	
- 2	113	141	M
1	157	130	M

8 K 15

- 7	40	130	M
- 4	69	137	M
- 1	267	262	
2	196	190	

9 K 15

- 6	79	123	M
- 3	199	239	
0	7	93	M

10 K 15

- 8	64	88	M
- 5	60	105	M
- 2	51	86	M

0 K 16

2	86	89	M
5	170	182	
8	117	179	

1 K 16

0	229	281	
3	269	298	
6	80	132	M

2 K 16

1	69	103	M
4	243	252	
7	559	545	

3 K 16

- 1	12	103	M
2	92	130	M
5	19	128	M

4 K 16

- 3	69	119	M
0	645	618	
3	63	133	M
6	65	88	M

5 K 16

- 2	79	130	M
1	12	135	M
4	268	289	

6 K 16

- 4	207	208	
- 1	14	135	M
2	33	124	M

7 K 16

- 6	32	133	M
- 3	12	135	M
0	101	126	M
3	153	157	

8 K 16

- 5	680	618	
- 2	139	126	M
1	19	95	M

9 K 16

- 7	62	105	M
- 4	322	295	
- 1	762	634	

10 K 16

- 6	64	88	M
- 3	53	77	M

0 K 17

1	11	177	M
4	116	170	M
7	63	132	M

1 K 17

2	100	293	
5	336	353	
8	39	77	M

2 K 17

0	66	172	M
3	110	245	
6	36	124	M

3 K 17

1	333	354	

4 K 17

- 1	64	179	M
2	11	161	M

5 K 17

- 3	785	832	
0	394	399	

6 K 17

1	185	274	

7 K 17

2	173	188	

8 K 17

0	111	103	M

0 K 18

1	275	327	
4	19	166	M
7	17	100	M

2 K 18

- 1	573	725	
2	75	166	M
5	546	578	

3 K 18

0	46	170	M

4 K 18

- 2	272	367	
1	23	166	M

5 K 18

2	86	133	M

6 K 18

0	349	318	

7 K 18

1	810	805	

0 K 19

2	642	670	
5	18	144	M

1 K 19

0	52	174	M
3	245	305	
6	499	397	

2 K 19

1	171	265	
4	120	137	M

3 K 19

- 1	414	467	
2	185	251	

4 K 19

0	160	157	M

5 K 19

1	119	141	M

6 K 19

2	44	147	

7 K 19

0	32	188	

0 K 20

1	124	305	
4	482	473	
7	51	64	M

1 K 20

2	50	247	
5	0	119	M

2 K 20

0	58	157	M
3	172	135	M

3 K 20

1	112	153	M

4 K 20

2	111	123	M

5 K 20

0	88	128	M

6 K 20

1	3	93	M

0 K 21

0	376	428	
3	371	361	
6	36	152	

1 K 21

1	58	152	M
4	537	533	

2 K 21

- 1	103	152	M
2	30	132	M
5	283	203	

3 K 21

0	40	139	M

4 K 21

1	66	121	M

5 K 21

2	150	137	

6 K 21

0	210	307	

0 K 22

2	182	245	
5	110	84	M

1 K 22

0	29	139	M
3	63	117	M

2 K 22

1	940	1121	
4	309	215	

3 K 22

2	94	169	

4 K 22

0	59	107	M

0 K 23

1	61	217	
4	103	77	M

1 K 23

2	301	310	

2 K 23

0	94	109	M
3	167	152	

3 K 23

1	245	224	

0 K 24

0	152	93	M

1 K 24

1	61	84	M

2 K 24

- 1	66	81	M

NOTES

M = UNOBSERVED REFLECTION. VALUE LISTED IS ESTIMATE OF MINIMUM OBSERVABLE.

X = OMITTED FROM REFINEMENT ON SUSPICION OF ABNORMAL ERROR OR MISIDENTIFICATION.

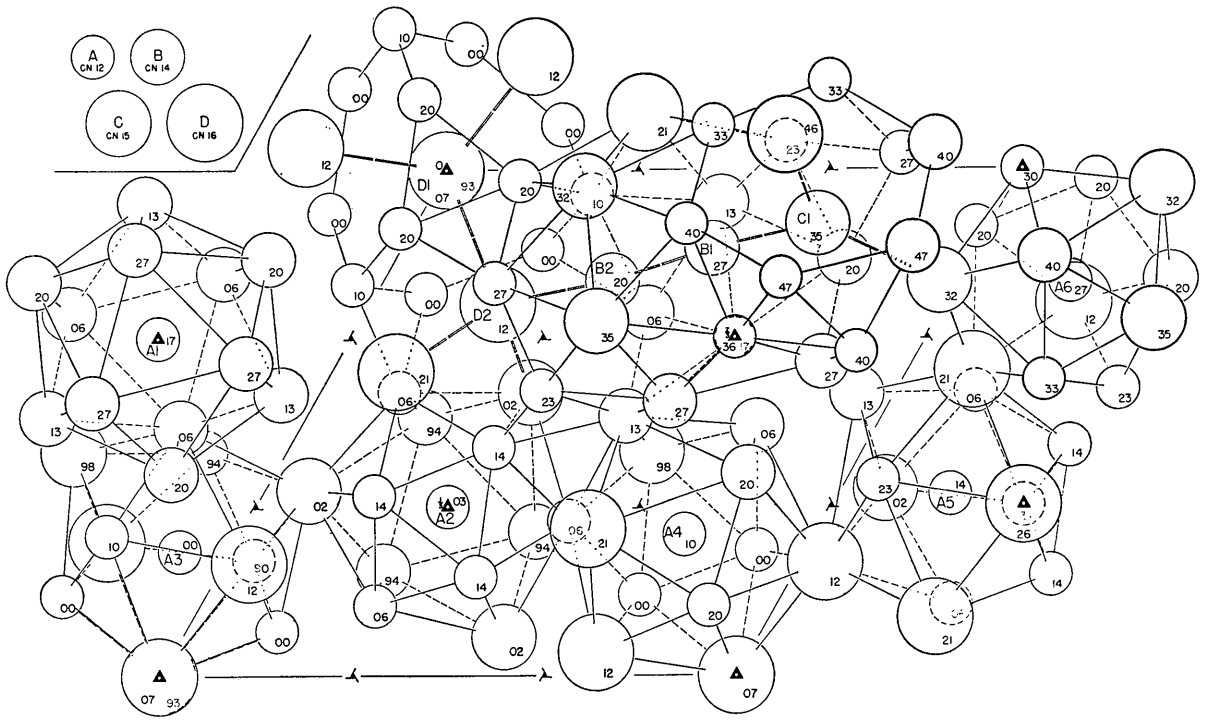

Fig. 3. *R* phase structure: atomic coordination. 6-coordinated ligands shown as double lines. For clarity many atoms (equivalent to other atoms shown) are omitted.

which yields a primitive cell. The basal plane of this cell is parallel to $(\bar{1}\bar{3}5)_{\text{hex.}}$ (equivalent to $(4\bar{1}5)_{\text{hex.}}$), very nearly the most strongly reflecting plane in the structure. The second order reflection, $(\bar{2},\bar{6},10)$ (or $(8,\bar{2},10)$), is also very strong. On this plane the cell edges are:

$$a_0'=9{\cdot}01,\quad b_0'=34{\cdot}01,\quad \gamma'=92^\circ\,59'.$$

For comparison the corresponding cell edges in the orthorhombic *P* phase and tetragonal σ phase are:

P	σ(Fe–Cr)
$a_0=9{\cdot}07$ Å	$a_0=8{\cdot}80$ Å
$b_0=16{\cdot}98$	

However, the **c**′ axis in the transformed cell is not even approximately orthogonal to the other two:

$$c_0'=9{\cdot}01\text{ Å},\quad \alpha'=23^\circ\,23{\cdot}6',\quad \beta'=74^\circ\,27{\cdot}5'.$$

The spacing of the 'main layers' (the interplanar spacing of $(\bar{1}\bar{3}5)$) is 2·17 Å, while in the *P* and σ phases it is one half the *c*-repeat, or 2·38 and 2·27 Å respectively.

The arrangement of the atoms lying on or close to the plane at $z'=\frac{1}{2}$ is roughly describable as a superstructure on a main layer of the *P* phase or the σ phase, as may be seen in Fig. 4. Much the same arrangement of hexagonal and pentagonal 'holes' is found in the greater part of the main layer ('kagomé tiling'; Frank & Kasper, 1959) as is found in the *P* phase. Over most of the cell the deviations of the main-layer atoms from $z=\frac{1}{2}$ are generally less than about 0·1 parameter unit, or 0·2 Å. There is, however, a region in the cell (where ligands are drawn with dashed lines in Fig. 4) which represents a transition from one unit cell to the next and the termination of linear rows of hexagonal and pentagonal 'holes'. In this transition region there are atoms between the 'main' and 'subsidiary' layers. Owing to the obliqueness of the **c**′ axis, these transition regions lie sandwiched between more-or-less normal main-layer regions. The higher-coordinated atoms, with their larger radii, tend to be concentrated in and around these transition regions.

The *R* phase structure resembles the μ phase structure (Arnfelt & Westgren, 1935) in being rhombohedral, though lower in symmetry and much more complicated than that structure (D^5_{3d}–$R\bar{3}m$, 13 atoms per rhombohedral unit cell). The μ phase and the Laves phases, like the *R* phase, possess strings of fused polyhedra along three-fold axes (see Fig. 5). Probably

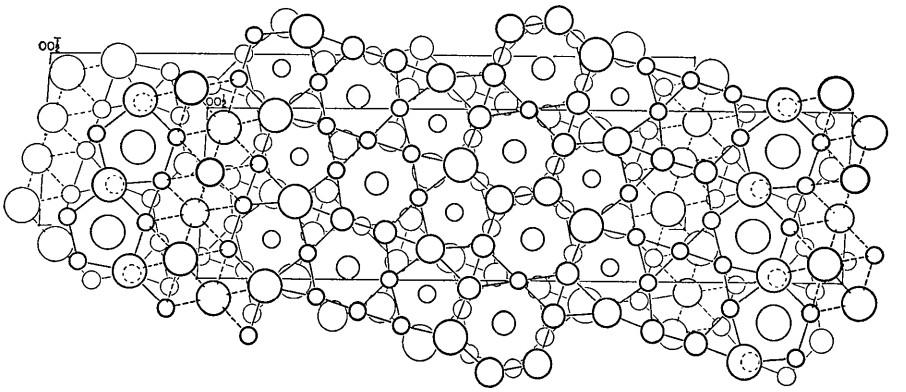

Fig. 4. R phase structure: normal projection on $(\bar{1}35)$, showing resemblance to P and σ phase structures. Dashed lines denote ligands to atoms not lying either in the main or in the subsidiary layers.

the most significant relationship of the R phase with the μ phase, as also with σ and P and other related phases, lies in the occurrence of coordination polyhedra with coordination numbers 12, 14, 15, and 16 (designated in the figures and tables as the respective types, A, B, C, D) and in the manner of their combination so as to yield packing that is essentially tetrahedral throughout (i.e., tetrahedral interstices only). These polyhedra have been discussed by Kasper (1956) in relation to complex alloy structures generally. They have been discussed in connection with the P and σ phase structures by Shoemaker, Shoemaker & Wilson (1957) and in connection with a number of structures including P and σ by Frank & Kasper (1958, 1959). As in the case of the other structures, the ligands in the R phase can be divided into two types, 5-coordinated and 6-coordinated; the latter being generally shorter, due in part perhaps to packing geometry but also, presumably, in part to stronger bonding. These are the types referred to by Frank & Kasper as 'minor' and 'major' ligands respectively.

The 6-coordinated ('major') ligands form a single three-dimensional network ('major skeleton') with branching at the 15- and 16-coordinated atoms, as shown in Fig. 6. In the fact that all atoms forming major ligands (coordinations 14, 15, 16) belong to a single all-pervading network, the R phase resembles the simple Laves phases ($MgCu_2$, $MgZn_2$ or FeW_2, $MgNi_2$), and differs from the more complex μ, σ and P phases in which unconnected networks exist with layering and/or interpenetration. The structure of the R phase network is, however, very complicated, and simple or meaningful relationships with those of the other structures are hard to find.

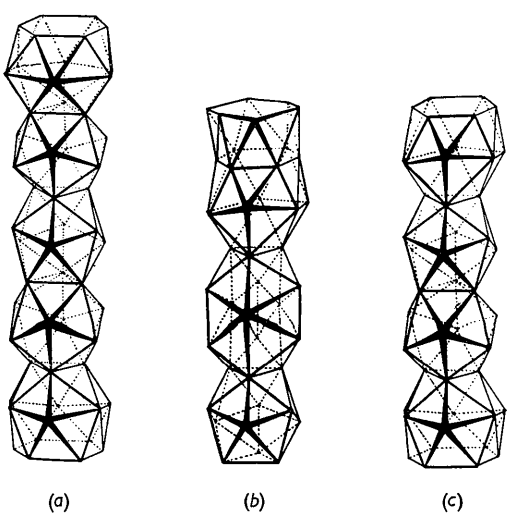

Fig. 5. R phase and some related structures: Strings of fused polyhedra along 3-fold axes. (*a*) R phase, entire *c*-repeat: CN 16, 12, 12, 12, 16. (*b*) μ phase, one-half *c*-repeat: CN 12, 15, 16, 14. (CN 12 is shared with lower half, below.) (*c*) $MgNi_2$, entire *c*-repeat: CN 16, 12, 12, 16).

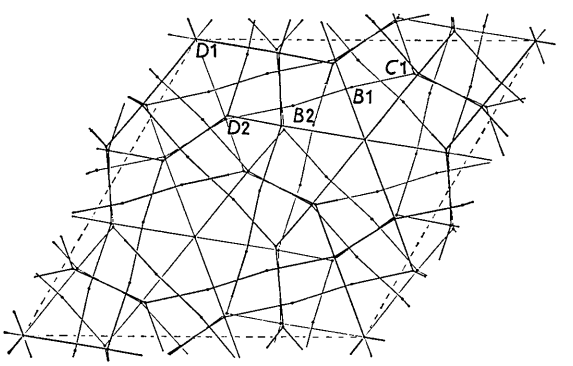

Fig. 6. R phase structure: Network of 6-coordinated ligands. Gradations in heaviness of lines increases with the hexagonal z coordinate from 0·00 to 1·00.

In this work, as in the work on the P phase, an attempt was made to deduce, from the interatomic distances, 5-coordinated and 6-coordinated radii for each kind of atom, by least-squares. The resulting radii, and their averages for each coordination type, are given in Table 5. 'Predicted' interatomic distances, calculated with these average radii, are given in Table 6, for comparison with the observed interatomic

distances, given in Table 4. The differences are somewhat larger than for the P and σ phases, averaging to 0·056 Å. in comparison to 0·036 Å for P and 0·039 Å for σ. The poorer agreement may be attributed in some part to lower precision in the interatomic distances, owing to the relatively scanty intensity data; however, it is significant that there are eight differences in excess of 0·1 Å, the largest being 0·174 Å, by contrast with only one, 0·122 Å, in the P phase. Moreover, this seems to be an inherent property of

Table 4. *Observed interatomic distances*

Atom	No.	R	pqr	D_o	Δ
			*A*1		
*B*1	6			2·629	−21
*B*2	6			2·635	−27
				Av.	24
			*A*2		
*A*5	3			2·528	−160
*A*6	3			2·417	−49
*B*1	3			2·478	130
*C*1	3			2·664	18
				Av.	89
			*A*3		
*A*3	2	$\bar{3}$		2·367	1
*A*4				2·352	16
*A*4′		$\bar{3}$		2·428	−60
*A*6		3^2	$12\bar{1}$	2·308	60
*B*1		3^2	$12\bar{1}$	2·592	16
*C*1		3	$12\bar{1}$	2·722	−40
*C*1′		$\bar{3}^5$	211	2·687	−5
*D*1				2·740	42
*D*1′		$\bar{1}$		2·780	2
*D*2				2·679	103
*D*2′		$\bar{3}^5$		2·765	17
				Av.	30
			*A*4		
*A*3				2·352	16
*A*3′		$\bar{3}^5$		2·428	−60
*A*5				2·322	46
*A*6		$\bar{3}$	$\bar{1}11$	2·303	65
*B*1		3^2	$12\bar{1}$	2·533	75
*B*2		3	$12\bar{1}$	2·537	71
*B*2′		$\bar{1}$	122	2·559	49
*C*1		3	$12\bar{1}$	2·774	−92
*D*1				2·852	−70
*D*2		3		2·818	−36
*D*2′		3	$\bar{1}11$	2·817	−35
*D*2″				2·757	25
				Av.	53
			*A*5		
*A*2				2·528	−160
*A*4				2·322	46
*A*5	2	3		2·455	−87
*A*6				2·428	−60
*A*6′		3		2·490	−122
*B*2		$\bar{1}$	122	2·560	48
*C*1				2·665	17
*D*1				2·765	17
*D*2		3		2·721	61
*D*2′		$\bar{3}$	$\bar{1}11$	2·674	108
*D*2″				2·763	19
				Av.	69

Atom	No.	R	pqr	D_o	Δ
			*A*6		
*A*2				2·417	−49
*A*3		3	211	2·308	60
*A*4		$\bar{3}^5$	211	2·303	65
*A*5				2·428	−60
*A*5′		3^2		2·490	−122
*B*1				2·576	32
*B*2		$\bar{1}$	122	2·570	38
*C*1		3^2		2·685	−3
*C*1′				2·673	9
*C*1″		$\bar{1}$	122	2·550	132
*D*2				2·857	−75
*D*2′		$\bar{1}$	211	2·738	44
				Av.	57
			*B*1		
*A*1				2·629	−21
*A*2				2·478	130
*A*3		3	211	2·592	16
*A*4		3	211	2·533	75
*A*6				2·576	32
*B*1	2	3^2		2·968	−120
*B*2				2·836	12
*B*2′		$\bar{3}$	003	2·814	34
*C*1				3·004	−82
*C*1′		$\bar{1}$	122	2·832	90
*D*2		3	211	3·063	−41
**B*2				2·382	42
**C*1		3^2		2·560	−41
				Av.	61
			*B*2		
*A*1				2·635	−27
*A*4		3^2	$\bar{1}11$	2·537	71
*A*4′		$\bar{1}$	122	2·559	49
*A*5		$\bar{1}$	122	2·560	48
*A*6		$\bar{1}$	122	2·570	38
*B*1		3		2·836	12
*B*1′		$\bar{3}^5$	003	2·814	34
*B*2	2	$\bar{3}$	003	2·881	−33
*C*1				2·958	−36
*C*1′		$\bar{1}$	122	2·912	10
*D*2		3	211	3·196	−174
**B*1				2·382	42
**D*2		$\bar{1}$	122	2·700	−52
				Av.	47

Table 4 (*cont.*)

Atom	No.	*R*	*pqr*	D_o	Δ
			*C*1		
*A*2				2·664	18
*A*3		3^2	$\bar{1}11$	2·722	−40
*A*3′		$\bar{3}$	$\bar{1}11$	2·687	−5
*A*4		3^2	$\bar{1}11$	2·774	−92
*A*5				2·665	17
*A*6		3		2·685	−3
*A*6′				2·673	9
*A*6″		$\bar{1}$	122	2·550	132
*B*1				3·004	−82
*B*1′		$\bar{1}$	122	2·832	90
*B*2				2·958	−36
*B*2′		$\bar{1}$	122	2·912	10
**B*1		3		2·560	−41
**C*1		$\bar{1}$	122	2·597	17
**D*2		$\bar{3}$	$\bar{1}11$	2·722	21
				Av.	41
			*D*1		
*A*3	3			2·740	42
*A*3′	3	$\bar{1}$		2·780	2
*A*4	3			2·852	−70
*A*5	3			2·765	17
**D*1	1	$\bar{1}$		2·843	29
**D*2	3			2·859	13
				Av.	29

Atom	No.	*R*	*pqr*	D_o	Δ
			*D*2		
*A*3				2·679	103
*A*3′		$\bar{3}$		2·765	17
*A*4		3^2		2·818	−36
*A*4′		$\bar{3}^5$	211	2·817	−35
*A*4″				2·757	25
*A*5		3^2		2·721	61
*A*5′		$\bar{3}^5$		2·674	108
*A*5″				2·763	19
*A*6				2·857	−75
*A*6′		$\bar{1}$	211	2·738	44
*B*1		3^2	$12\bar{1}$	3·063	−41
*B*2		3^2	$12\bar{1}$	3·196	−174
**B*2		$\bar{1}$	122	2·700	−52
**C*1		$\bar{3}^5$	211	2·722	21
**D*1				2·859	13
**D*2		$\bar{1}$	211	2·868	4
				Av.	52
				Overall weighted average	56

Atom: Designation of near neighbor. Primes distinguish among non-equivalently disposed neighbors of the same crystallographic kind.
No.: Number of equivalently disposed neighbors of that kind, if different from unity.
R, *pqr*: Operation by which the neighbor is obtained from the one with coordinates listed in Table 2. *R* is the rotation or rotatory inversion or inversion, and *pqr* represents a *subsequent* translation $p/3, q/3, r/3$.
D_o: Interatomic distances in Å calculated from parameters given in Table 2.
Δ: Amount in units of 0·001 Å, by which the predicted distance (Table 6) differs from D_o.

the structure, inasmuch as attempts to 'refine' the parameters without intensity data gave substantially the same large differences.

Table 5. *Summary of radii*

Atom	No.	*r*	*r**
*A*1	1	1·208 Å	
*A*2	2	1·198	
*A*3	6	1·174	
*A*4	6	1·180	
*A*5	6	1·198	
*A*6	6	1·176	
A	27	1·184	
*B*1	6	1·422	1·210 Å
*B*2	6	1·426	1·215
B	12	1·424	1·212
C	6	1·498	1·307
*D*1	2	1·603	1·419
*D*2	6	1·597	1·442
D	8	1·598	1·436
Total	53		

Nevertheless the agreement is good enough to corroborate the indication obtained with the σ and *P* phase results that the ligand radii should conform in considerable degree to the symmetry of the idealized coordination polyhedron, and should be essentially constant for a given atom coordination and given ligand coordination. As with the *P* phase the coordination type is in part determined by atomic size, as shown by the indications that the more highly coordinated sites are occupied predominantly by molybdenum atoms.

Table 6. *Predicted interatomic distances*

A–*A*	2·368 Å	**B*–*B*	2·424 Å
A–*B*	2·608	**B*–*C*	2·519
A–*C*	2·682	**B*–*D*	2·648
A–*D*	2·782		
B–*B*	2·848	**C*–*C*	2·614
B–*C*	2·922	**C*–*D*	2·743
B–*D*	3·022		
		**D*–*D*	2·872

The results of this and previous investigations give some ground for new speculations as to the filling of atomic orbitals or energy bands in structures of these types. It is possibly significant that the degeneracy of the *d* orbitals is not removed under the symmetry group (Y_h) of the regular icosahedron. This fact suggests that in the coordination 12 atoms the *d* band prefers to be substantially filled (or perhaps in some

cases substantially empty). These sites tend to be occupied by elements at and to the right of Mn, and the atoms would be somewhat negative by electron transfer. In the other coordinations the *d* degeneracy is removed, and *d*, *s*, and *p* orbitals might be expected to hybridize to form directed bonds in the 6-coordinated ligand directions. These sites tend to be occupied by elements at and to the left of Cr and Mo (Kasper & Waterstrat, 1956), with Mo replacing Cr in the higher coordinations because of larger size; these atoms would then be somewhat positive by electron transfer. These considerations will be discussed more in detail elsewhere (Shoemaker, 1960).

Some preliminary single-crystal exploration was done by Dr Clara B. Shoemaker; reference to her photographs materially aided in the establishment of the monocrystallinity of the crystal fragment which we used. Mr Paul Metzger assisted with the refinement of the lattice constants with powder data.

We wish to thank Prof. Paul A. Beck of the University of Illinois for supplying us with *R* phase specimens and for much helpful assistance and discussion. We gratefully acknowledge the use of the IBM 704 at the MIT Computation Center, and wish to thank Prof. Vladimir Vand of Pennsylvania State University for Programming and operating suggestions. We are also happy to acknowledge the financial support of the Office of Ordnance Research.

References

ARNFELT, H. & WESTGREN, A. (1935). *Jernkontor. Ann.* **119**, 185.
BERGMAN, G. & SHOEMAKER, D. P. (1954). *Acta Cryst.* **7**, 857.
DARBY, J. B. JR., DAS, B. N., SHIMOMURA, Y. & BECK, P. A. (1958). *Trans. Amer. Inst. Min. (Metall.) Engrs.* **212**, 235.
DAUBEN, C. H. & TEMPLETON, D. H. (1955). *Acta Cryst.* **8**, 841.
FRANK, F. C. & KASPER, J. S. (1958). *Acta Cryst.* **11**, 184.
FRANK, F. C. & KASPER, J. S. (1959). *Acta Cryst.* **12**, 483.
KASPER, J. S. (1956). *Theory of Alloy Phases*, p. 264. Amer. Soc. of Metals Symposium.
KASPER, J. S. & WATERSTRAT, R. M. (1956). *Acta Cryst.* **9**, 289.
KOMURA, Y., SHOEMAKER, D. P. & SHOEMAKER, C. B. (1957). *Acta Cryst.* **10**, 774.
RIDEOUT, S., MANLY, W. D., KAMEN, E. L., LEMENT, B. S. & BECK, P. A. (1951). *Trans. Amer. Inst. Min. (Metall.) Engrs.* **191**, 872.
SHOEMAKER, D. P. (1960). *Acta Metall.* (To be published.)
SHOEMAKER, D. P., SHOEMAKER, C. B. & WILSON, F. C. (1957). *Acta Cryst.* **10**, 1.
THOMAS, L. H. & UMEDA, K. (1957). *J. Chem. Phys.* **26**, 293.

Acta Cryst. (1960). **13**, 585

X-Ray Diffraction Studies of the δ Phase, Mo–Ni*

BY CLARA B. SHOEMAKER, ALWYN H. FOX†, AND DAVID P. SHOEMAKER

Department of Chemistry, Massachusetts Institute of Technology, Cambridge, Massachusetts, U.S.A.

(*Received* 19 *June* 1959 *and in revised form* 18 *December* 1959)

Single-crystal X-ray diffraction studies of the δ phase, Mo–Ni (61·1 weight percent Mo) have shown that it is at least pseudotetragonal, with $a_0 = 9{\cdot}108$, $c_0 = 8{\cdot}852$ Å, and extinctions suggesting space group D_4^6–$P4_22_12$. There are, however, a few cases of differing intensity between (*hkl*) and (*khl*), indicating a reduction of the true Laue symmetry to D_{2h}; the true space group is perhaps $P2_12_12$ or $P2_12_12_1$. The (0*kl*) and (*h*0*l*) weighted reciprocal lattice nets closely resemble the (*hk*0) net of the σ phase. All attempts to determine the structure in detail were unsuccessful.

Introduction

In connection with work in these laboratories on the crystal structures of the *P* phase, Mo–Ni–Cr (Shoemaker, Shoemaker & Wilson, 1957) and the *R* phase Mo–Co–Cr (Komura, Sly & Shoemaker, 1960), we undertook to investigate the crystal structure of the δ phase, Mo–Ni, discovered by Ellinger (1942). This phase appeared to be closely related to the σ phase (Bergman & Shoemaker, 1954) and to the *P* phase, as was demonstrated clearly in the work of Beck and coworkers (Rideout *et al.*, 1951) who found σ, *P*, and δ phase regions arranged in a roughly linear row on the Mo-Ni-Cr phase diagram at 1200 °C. The δ phase in the Mo–Ni system exists at the approximate atomic ratio 1:1, in the range 61 to 63 weight percent molybdenum.

Experimental

A specimen of this alloy, annealed at 1200 °C., was kindly supplied by Prof. Paul A. Beck of the Univer-

* Sponsored by Office of Ordnance Research. Computations were done in part at the MIT Computation Center, in part on X-RAC at Pennsylvania State University.

† Present address: Mullard Research Laboratories, Salfords, Redhill, England.